AAC Journals.ASM.org

Discovery of a Novel Class of Boron-Based Antibacterials with Activity against Gram-Negative Bacteria

Vincent Hernandez,[a] Thibaut Crépin,[b] Andrés Palencia,[b] Stephen Cusack,[b] Tsutomu Akama,[a] Stephen J. Baker,[a] Wei Bu,[a] Lisa Feng,[a] Yvonne R. Freund,[a] Liang Liu,[a] Maliwan Meewan,[a] Manisha Mohan,[a] Weimin Mao,[a] Fernando L. Rock,[a] Holly Sexton,[a] Anita Sheoran,[a] Yanchen Zhang,[a] Yong-Kang Zhang,[a] Yasheen Zhou,[a] James A. Nieman,[c] Mahipal Reddy Anugula,[c] El Mehdi Keramane,[c] Kingsley Savariraj,[c] D. Shekhar Reddy,[c] Rashmi Sharma,[c] Rajendra Subedi,[c] Rajeshwar Singh,[c] Ann O'Leary,[d] Nerissa L. Simon,[e] Peter L. De Marsh,[e] Shazad Mushtaq,[f] Marina Warner,[f] David M. Livermore,[f,g] M. R. K. Alley,[a] Jacob J. Plattner[a]

Anacor Pharmaceuticals Inc., Palo Alto, California, USA[a]; European Molecular Biology Laboratory, Grenoble Outstation, and Unit of Virus Host-Cell Interactions, UJF-EMBL-CNRS, UMI 3265, Grenoble, France[b]; NAEJA Pharmaceuticals Inc., Edmonton, Alberta, Canada[c]; Ricerca, Concord, Ohio, USA[d]; Antibacterial Discovery Performance Unit, GlaxoSmithKline, Collegeville, Pennsylvania, USA[e]; Antibiotic Resistance Monitoring & Reference Laboratory, Health Protection Agency Microbiology Services-Colindale, London, United Kingdom[f]; Norwich Medical School, University of East Anglia, Norwich, United Kingdom[g]

Gram-negative bacteria cause approximately 70% of the infections in intensive care units. A growing number of bacterial isolates responsible for these infections are resistant to currently available antibiotics and to many in development. Most agents under development are modifications of existing drug classes, which only partially overcome existing resistance mechanisms. Therefore, new classes of Gram-negative antibacterials with truly novel modes of action are needed to circumvent these existing resistance mechanisms. We have previously identified a new a way to inhibit an aminoacyl-tRNA synthetase, leucyl-tRNA synthetase (LeuRS), in fungi via the oxaborole tRNA trapping (OBORT) mechanism. Herein, we show how we have modified the OBORT mechanism using a structure-guided approach to develop a new boron-based antibiotic class, the aminomethylbenzoxaboroles, which inhibit bacterial leucyl-tRNA synthetase and have activity against Gram-negative bacteria by largely evading the main efflux mechanisms in *Escherichia coli* and *Pseudomonas aeruginosa*. The lead analogue, AN3365, is active against Gram-negative bacteria, including *Enterobacteriaceae* bearing NDM-1 and KPC carbapenemases, as well as *P. aeruginosa*. This novel boron-based antibacterial, AN3365, has good mouse pharmacokinetics and was efficacious against *E. coli* and *P. aeruginosa* in murine thigh infection models, which suggest that this novel class of antibacterials has the potential to address this unmet medical need.

The rise in the prevalence of resistance to the frontline Gram-negative antibacterials (1–3) is disturbing, as Gram-negative organisms cause the majority of infections in hospital intensive care units (4). This increase in resistance has led to a wider use of carbapenems, which are now being threatened by Gram-negative bacteria bearing the carbapenemases NDM-1 (5), KPC (6), and OXA-48 (7). The result is that the polymyxins B and E (colistin) have seen a widespread reintroduction into clinical practice (8) after having been abandoned in the 1970s due to concerns about their nephrotoxicity and neurotoxicity. Resistance to polymyxins is even now increasing, especially in *Klebsiella pneumoniae* (9). To date, treatment of Gram-negative antibacterial infections has relied largely on antibacterial monotherapy which inhibits more than one target, for example, topoisomerase II and IV, penicillin-binding proteins (PBP), and the ribosome. However, the reservoir of resistance genes has blunted the advantage of traditional multitargeting monotherapeutics to the point where the antibiotic pipeline for Gram-negative bacteria is worse than for tuberculosis (TB), a neglected bacterial disease, which has few if any multigene targets. Furthermore, no new PBP inhibitor is being advanced into the clinic without an accompanied beta-lactamase inhibitor. This lack of new agents is extremely worrisome and has led to the use of even rifampin, which inhibits a single gene target, in combination therapy, for example, in the treatment of multidrug-resistant (MDR) *Acinetobacter baumannii* and *Pseudomonas aeruginosa* infections (10). In order to address this unmet medical need, we have identified a new class of antibacterials that inhibits a novel target, the editing site of leucyl-tRNA synthetase (LeuRS), which bypasses existing resistance mechanisms to established antibiotics in Gram-negative bacteria.

Aminoacyl-tRNA synthetases (AARS) are a family of essential enzymes required for protein synthesis that have been underutilized as targets for antimicrobials. Mupirocin, an isoleucyl-tRNA synthetase inhibitor, is the only antibiotic used in the clinic that targets an AARS, but its narrow antibacterial spectrum and poor systemic pharmacokinetics make it suitable for only the topical treatment of staphylococcal and streptococcal skin infections (11). We have recently shown that the antifungal tavaborole (AN2690) specifically inhibits *Saccharomyces cerevisiae* cytoplasmic LeuRS by an oxaborole tRNA trapping (OBORT) mechanism (12). The LeuRS enzyme ensures the fidelity of translation by means of a proofreading mechanism (13), which involves translocation of the 3′-aminoacylated end of $tRNA^{Leu}$ from the synthetic active site to a separate editing active site 30 Å away, where any mischarged tRNAs are hydrolyzed (14). When tavaborole

Received 9 October 2012 **Returned for modification** 5 November 2012
Accepted 22 December 2012
Published ahead of print 7 January 2013
Address correspondence to M. R. K. Alley, dalley@anacor.com.
Supplemental material for this article may be found at http://dx.doi.org/10.1128/AAC.02058-12.

doi:10.1128/AAC.02058-12
The authors have paid a fee to allow immediate free access to this article.

TABLE 1 X-ray data collection and refinement statistics

Parameter	AN2679	AN3016	AN3017	AN3213
Data collection				
Space group	$P2_12_12_1$	$P2_12_12_1$	$P2_12_12_1$	$P2_1$
Cell dimensions (Å)	a = 76.18, b = 118.94, c = 141.03	a = 76.68, b = 119.96, c = 142.73	a = 76.90, b = 118.80, c = 140.40	a = 89.37, b = 76.94, c = 90.71, β= 102.37°
Resolution (Å)	2.1	2.4	2.2	2.3
R_{sym}[a] (%)	5.6 (36.7)	9.1 (52.9)	6.7 (46.1)	6.3 (57.5)
$I/\sigma I$[a]	20.1 (3.0)	13.1 (2.4)	13.7 (2.9)	16.8 (2.5)
Completeness[a] (%)	96.5 (75.0)	98.7 (99.2)	99.7 (99.8)	99.9 (99.9)
Redundancy	3.90	3.33	3.99	3.75
Refinement				
Resolution[a] (Å)	90.9–2.08 (2.14–2.08)	98.8–2.40 (2.46–2.40)	90.5–2.20 (2.25–2.20)	88.7–2.31 (2.37–2.31)
No. of reflections work (free)	71,134 (3,759)	49,003 (2,645)	62,461 (3,333)	50,171 (2,693)
R_{work}[a] (%)	19.4 (26.8)	20.8 (28.7)	20.6 (26.1)	20.0 (29.5)
R_{free}[a] (%)	24.7 (30.8)	26.0 (37.7)	25.0 (31.7)	24.7 (35.7)
Total no. of non-hydrogen atoms	8,590	8,359	8,570	8,709
No. of protein atoms	6,803	6,517	6,526	6,469
No. of tRNA atoms	1,447	1,710	1,756	1,818
No. of ions and ligand atoms:				
Mg	3	2	3	0
Inhibitor	9	14	11	16
No. of water molecules	328	116	274	406
Average B-factor (Å^2)	28.8	43.8	33.7	38.4
RMS deviations				
Bond length deviations from ideal (Å)	0.014	0.014	0.014	0.012
Bond angle deviations from ideal (°)	1.624	1.390	1.361	1.458

[a] Values for highest-resolution shells are shown in parentheses.

binds to the LeuRS editing active site, the boron atom in the oxaborole ring bonds to the *cis*-diols of the terminal ribonucleotide of $tRNA^{Leu}$, forming an adduct that traps the 3′ end of $tRNA^{Leu}$ in the editing site, thereby preventing its translocation to the synthetic active site. This blocks $tRNA^{Leu}$ from being aminoacylated, which ultimately leads to the inhibition of protein synthesis (12). We have used this mechanism in combination with chemistry, biochemistry, X-ray crystallography, and microbiology to synthesize LeuRS inhibitors with *in vitro* and *in vivo* activity against Gram-negative bacteria, including multidrug-resistant isolates.

MATERIALS AND METHODS

Chemical synthesis. Starting materials used were either available from commercial sources or prepared according to literature procedures and had experimental data in accordance with those reported. The synthesis of AN3016, AN3017, AN3334, AN3213, AN3365, AN3376, and AN3377 is described in detail in the supplemental material.

Crystallography. Preparation of *Escherichia coli* LeuRS and T7 transcripts of $tRNA_5^{Leu}$(UAA) are described elsewhere (15). *E. coli* LeuRS-$tRNA^{Leu}$-benzoxaborole ternary complexes were crystallized by mixing 2 μl of complex solution with 2 μl of a crystallization solution and then equilibrating by hanging drop pour diffusion against 500 μl of reservoir solution. Crystals appeared at 293 K within 4 to 5 days in 14 to 18% polyethylene glycol 6000 (PEG 6000), 200 mM NaCl, and 0.1 M sodium acetate at pH 5.6. For data collection, these crystals were briefly transferred to 1 μl of reservoir solution containing 22% (wt/vol) ethylene glycol and then flash-cooled in liquid nitrogen. Diffraction data were collected at 100 K at the European Synchrotron Radiation Facility (ESRF; Grenoble, France). Crystals were either of space group $P2_12_12_1$ or $P2_1$, with one molecule complex per asymmetric unit. Data sets were integrated and scaled using the XDS suite (16). Subsequent data analysis was performed with the CCP4 suite (17). Structures were solved by molecular replacement (18), using the *E. coli* LeuRS-tRNA complex (15) structure as a search model. A more detailed description of the *E. coli* LeuRS-$tRNA^{Leu}$ structure is presented elsewhere (15). Models were built with COOT (19) and refined by rigid-body refinement, followed by isotropic B-factor refinement using REFMAC5 with TLS (20). Electron density for the different benzoxaboroles covalently linked to the 3′ end of the tRNA was clearly visible. The crystallographic data collection and refinement statistics are presented in Table 1.

Human cytoplasmic LeuRS expression. An *E. coli* codon-optimized human cytoplasmic LeuRS gene was synthesized by GenScript Inc. with an N-terminal six-histidine tag. This LeuRS construct had the C-terminal 58 amino acids removed to improve expression of a functional LeuRS in *E. coli*. Ling et al. have shown previously that enzyme activity is retained even with an 85-amino-acid deletion (21). The protein was overexpressed and purified to 0.226 mg/ml by GenScript Inc.

LeuRS aminoacylation assay. Unless stated otherwise, compound, *E. coli* LeuRS (22), and *E. coli* total tRNA (Roche) were preincubated for 20 min in 50 mM HEPES-KOH (pH 8.0), 30 mM $MgCl_2$, 30 mM KCl, 0.02% (wt/vol) bovine serum albumin, and 1 mM dithiothreitol with 20 μM [^{14}C]leucine (306 mCi/mmol; Perkin-Elmer) at 30°C. In assays with human cytoplasmic LeuRS, crude baker's yeast tRNA (Roche) and 0.4 μM [^{3}H]leucine (144.2 mCi/mmol; Perkin-Elmer) were used instead of the *E. coli* tRNA and [^{14}C]leucine. Reactions were started by the addition of 4 mM ATP and, at specific times, tRNA was precipitated by the addition of 10% (wt/vol) trichloroacetic acid (TCA), recovered by filtration (Millipore Multiscreen; MSHAN4B50), washed with 5% TCA (wt/vol), and counted by a Wallac MicroBeta Trilux model 1450 liquid scintillation counter.

LeuRS reactivation rate determination. To establish the reversibility of inhibition, 40 nM *E. coli* LeuRS and sufficient tRNA and compound were preincubated for 1 h at 4°C to inhibit 90% of the enzyme's activity (~10× 50% inhibitory concentration [IC_{50}]). LeuRS inhibitor complexes were then diluted 200-fold, and enzyme activity was determined at various time intervals, as described above. Compound reactivation rates were determined by fitting the LeuRS activity reactivation curves using a one-phase exponential decay model with the GraphPad Prism Program (La Jolla, CA).

MIC determination. MIC values were predominately determined using the CLSI broth microdilution method for aerobic and anaerobic bacteria (23, 24). MIC values were determined at least twice on separate days, with the higher value used to represent the MIC value.

Macromolecular synthesis assay. Overnight cultures of *E. coli* ATCC 25922 were diluted 1,000-fold in M9 medium with 0.25% (wt/vol) yeast extract and allowed to grow to an A_{600} of ~0.3. The culture was incubated at 37°C for 20 min with either 2.5 μCi/ml [^{14}C]leucine to measure protein synthesis, 1.0 μCi/ml [^{14}C]thymidine for DNA synthesis, 0.5 μCi/ml [^{14}C]uridine for RNA synthesis, 5.0 μCi/ml [^{14}C]acetic acid for fatty acid synthesis, or 1.0 μCi/ml [^{14}C]*N*-acetylglucosamine for cell wall synthesis, with increasing concentrations of AN3365. Four antibacterial agents (tetracycline, rifampin, ciprofloxacin, and triclosan) with known mechanisms of action were tested as controls. Duplicate samples of 40 μl were precipitated with TCA at 20 min after compound addition and added to 100 ml of ice-cold 20% (wt/vol) TCA. After 60 min on ice, the samples were collected over vacuum on a 96-well glass fiber filter plate (Millipore MSFBNB50) and washed three times with 150 μl of ice-cold 10% (wt/vol) TCA. A 40-μl aliquot of scintillation cocktail was added to the dried filter plate, and counts were obtained in a MicroBeta Trilux 1450 scintillation counter (PerkinElmer).

Time-kill studies. *E. coli* ATCC 25922 and *P. aeruginosa* ATCC 27853 were obtained from freshly cultured LB plates and grown overnight at 37°C with shaking in 5 ml of cation-adjusted Mueller-Hinton broth (CA-MHB). To prepare the inoculum, the overnight culture was diluted 1:100 in 3 ml of CA-MHB and grown for 1 to 2 h at 37°C with shaking to obtain log-phase cells. The bacteria were then inoculated at approximately 5×10^5 CFU/ml into CA-MHB, and antibiotics were added at 4- and 10-fold the MIC. Samples were taken at various times over 24 h, and serial dilutions were plated on LB plates for CFU determination. Each experiment was repeated at least twice, and representative data from one such experiment are shown.

Resistance frequency and DNA sequencing of *leuS* mutants. Resistance mutants were obtained by plating cells on CA-MHB Noble agar plates containing either 4-fold or 10-fold the MIC of AN3365 or comparators. Colonies were counted after 48 h of incubation at 37°C. The resistance of these colonies was confirmed by their ability to grow on plates containing AN3365 or comparators at either 4-fold or 10-fold the MIC. The frequency of resistance was determined by dividing the number of resistant mutants by the total number of cells plated as determined by plating dilutions of the overnight culture on LB plates. Sequencing of the *leuS* gene was performed by Sequetech Corporation (Mountain View, CA).

Allelic exchange. The DNA from an AN3365-resistant mutant of *P. aeruginosa* ATCC 27853 with the amino acid substitution T252P in the editing domain of LeuRS was used as a template to amplify *leuS*. The 5′ end of the mutant *leuS* gene was amplified by Phusion high-fidelity DNA polymerase (NEB) using primers GCGgagctcTCGCGCGTTGCAGCTC AGCC and GCGgagctcAGTAGGTATCGGCGACCACC (lowercase indicates restriction enzyme site). The amplified product was cloned into pRE107GM via the primer-introduced SacI sites. Plasmid pRE107GM was constructed by replacing the PstI fragment containing the ampicillin resistance gene in pRE107 (25) with a PstI fragment containing the gentamicin resistance gene from pDAH257 (26) using the *E. coli* strain EC100D *pir-116* that supports R6K replication (Epicentre). Cloning of the 5′ portion of the *leuS* gene bearing the T252P mutation into pRE107GM resulted in plasmid pRE107GMP3, which was then conjugated into *P. aeruginosa* ATCC 27853 by a triparental mating using DH10B bearing the plasmid pRK2013 (27). *P. aeruginosa* ATCC 27853 transconjugants were selected by their gentamicin and chloramphemicol resistance, and their sensitivity to 5% (wt/vol) sucrose was confirmed. These transconjugants were plated out on LB agar containing 5% sucrose (Teknova, CA), and the sucrose-resistant colonies were tested for resistance to AN3365. The *leuS* gene from the AN3365-resistant sucrose-resistant colonies was sequenced to confirm the presence of the T252P mutation.

***In vitro* cytotoxicity measurements.** Overnight cultures were treated with the compound and incubated at 37°C for 24 h with 5% CO_2. An aliquot of 20 μl/well of Cell Titer 96 AQueous One Solution reagent (MTS tetrazolium compound; Promega, Madison, WI) was added to the cells, and the plates were further incubated for 2.5 h at 37°C with 5% CO_2. Absorbance was measured at 490 nm and 690 nm in a Molecular Devices plate reader (Sunnyvale, CA), and the 690-nm readings were subtracted from the 490-nm readings. Cycloheximide, a eukaryotic cytoplasmic protein synthesis inhibitor, was used as a positive control and had an IC_{50} of 0.6 μM.

Mouse pharmacokinetic analysis. The studies were conducted using female CD-1 mice with a body weight of 23 to 28 g. On the morning of dosing, mice were split randomly into 3 dosing groups to receive test article solution in sterile water, adjusted to pH 5.02 with 1 N NaOH at a dose level of 30 mg/kg by either tail vein injection (i.v.; $n = 27$), oral gavage (p.o.; $n = 24$), or subcutaneous injection (s.c.; $n = 24$). After mice were dosed, blood samples were collected via cardiac puncture at specific time points ($n = 3$ mice/time point) through 24 h (K_2EDTA as the anticoagulant) and processed for plasma. Antibiotic concentrations in the plasma samples were analyzed by liquid chromatography-tandem mass spectrometry (LC-MS/MS). The LC-MS/MS analysis was conducted using internal standard/peak area methods. The limit of quantitation (LOQ) was 2 ng/ml. Pharmacokinetic analyses of the mean plasma concentration-time profiles were performed using WinNonlin Pro version 5.2. A compartmental model was used for the i.v. data, and the noncompartmental model was used for p.o. and s.c. data. The time-concentration curve after an i.v. dose showed a biexponential decline with first-order elimination.

Mouse plasma protein binding determination. Compounds were added to 1.5-ml aliquots of mouse plasma and plasma ultrafiltrate to concentrations of 1 μg/ml and 10 μg/ml and then incubated in a shaking water bath at 37°C for 15 min. Both samples were treated similarly, and a 0.5-ml aliquot was removed from each tube and added to the filter reservoir of the Microcon centrifugal filter devices (Ultracel YM-30; molecular weight cutoff = 30 kDa; Bedford, MA). The devices were centrifuged at 1,000 × *g* for 10 min, and 100 μl of filtrate was transferred to the 96-well plate and diluted 5-fold. Ten-microliter volumes of the samples were injected and analyzed with the LC-MS/MS system. All samples were analyzed in duplicate. Quantitation was based on peak areas, and all integrations were performed with peak areas using Analyst version 1.4.1 (Applied Biosystems, Foster City, CA). Plasma protein binding was calculated based on the following equation: plasma protein binding (%) = [(peak area of spiked plasma ultrafiltrate − peak area of filtrate plasma)/peak area of spiked plasma ultrafiltrate] × 100.

Neutropenic murine thigh infection model. Colonies from an overnight culture on Trypticase soy agar (TSA) were transferred to sterile phosphate-buffered saline (PBS) and diluted to the optimized concentration for injection of each bacterium, which was 1.9×10^5 CFU for *E. coli* ATCC 25922, 2.8×10^6 CFU for *E. coli* ANA598, and 3.0×10^5 CFU for *P. aeruginosa* ATCC 27853. A serial dilution of the inoculum was plated out on TSA, and the number of CFU was determined after overnight incubation at 37°C. Female CD-1 mice weighing between 19 and 28 g (Charles River Laboratories, Portage, MI) were made neutropenic with intraperitoneal injections of cyclophosphamide (150 mg/kg of body weight in a 10-ml/kg volume) on days −4 and −1 before bacterial inoculation. Each animal was inoculated with 0.1 ml of bacteria into the thigh muscle of each

Compound	AN2679	AN3017	AN3334	AN3376	AN3016	AN3213	AN3377	AN3365
E. coli LeuRS IC_{50} (μM)	27.5	2.3	1.0	48.0	2.1	0.54	87.2	0.31

FIG 1 Chemical structures and biochemical activity. The IC_{50} values were determined by preincubating the compounds with crude *E. coli* tRNA, *E. coli* LeuRS enzyme, and ^{14}C-leucine for 20 min, before adding ATP to start the reaction. All reactions were performed in triplicate, and the mean values were used to determine an IC_{50} using Prism 4 (GraphPad). AN3334 is also known as ABX.

hind leg. Test compounds and control agent (tobramycin) were administered in sterile saline at 2 h after infection, and additional doses were administered according to the specific study protocols. Thighs from the hind legs of each mouse were collected at 2 h (untreated control mice) and 24 h postinfection and homogenized, and 10-fold serial dilutions were plated on TSA. The CFU were counted after overnight incubation at 37°C, and the number of CFU/g thigh was determined. Each test group consisted of at least four mice.

Immunocompetent murine thigh infection model. A culture of *P. aeruginosa* 1161949 was shaken overnight (120 rpm) in brain heart infusion (BHI) broth at 37°C and then washed twice by centrifugation and resuspended in BHI medium. A 1-cm length of chromic gut suture (3.0) was washed in saline and then incubated with this culture for 1 h at 37°C. Mice were anesthetized (80 mg/kg ketamine and 5 mg/kg xylazine i.p.), a 1-cm incision was made in the inguinal area to expose the thigh muscles, and a single section of suture containing *P. aeruginosa* was inserted into the deep thigh musculature. The incision was closed with a surgical staple, and the mice were dosed with a single injection of banamine (1 mg/kg) for pain relief. Groups of mice were treated with vehicle (water), AN3365, or ceftazidime twice daily for 4 days and euthanized 17 h after the final dose. The suture and surrounding tissue were aseptically removed and mechanically homogenized in saline. Ten-fold serial dilutions were plated onto MacConkey agar plates in triplicate. Plates were incubated overnight at 37°C, and colonies were counted to enumerate CFU/thigh.

Protein structure accession numbers. Protein Data Bank (PDB) accession numbers are as follows: for AN3016, 3ZJU; for AN3017, 3ZJT; for AN3213, 3ZJV; and for AN2679, 4ARI.

RESULTS AND DISCUSSION

Addition of 3-aminomethyl to the core benzoxaborole improves activity. Although the core benzoxaborole, AN2679, has poor biochemical activity versus *Escherichia coli* LeuRS (Fig. 1), we managed to cocrystallize AN2679 with *E. coli* LeuRS and tRNA^{Leu}. AN2679 was bound only in the editing active site (Fig. 2A), with the boron atom forming bonds to the *cis*-diols on the terminal adenosine ribonucleotide of tRNA^{Leu} (Fig. 2B). An overlay of the *Thermus thermophilus* LeuRS editing substrate analogue 2′-(L-norvalyl)amino-2′-deoxyadenosine (Nva2AA) cocrystal structure (14) with the AN2679 cocrystal structure showed that this benzoxaborole missed key interactions (Fig. 2C). The amino group of Nva2AA makes key interactions with Asp342, Asp345, and the carbonyl of Met336 in the amine-binding pocket in the editing active site (Fig. 2C). Molecular modeling suggested that an aminomethyl substitution should be added to position 3 on AN2679 to gain these interactions. Therefore, the 3-aminomethyl-substituted benzoxaborole was synthesized to create AN3017, which had a half-maximum inhibitory concentration (IC_{50}) for *E. coli* LeuRS that was 10-fold more potent than that of AN2679 (Fig. 1). As predicted from the docking analysis, the cocrystal structure of AN3017 (Fig. 3A) showed that its amino group was within hydrogen-bonding distance to Asp342, Asp345, and the carbonyl of Met336 in the amine pocket, which matched the amine interactions observed with Nva2AA. Since only the *S*-stereoisomer in the AN3017 racemate mixture was observed in the cocrystal structure, we isolated both enantiomers by separation of a synthetic intermediate using chiral high-performance liquid chromatography (HPLC) followed by removal of the *tert*-butyl carbamate-protecting group to yield AN3334 and AN3376. As expected, the *S*-stereoisomer, AN3334, was more active with an IC_{50} of 1.0 μM than with 48 μM for AN3376, the *R*-stereoisomer (Fig. 1). AN3334 had good antimicrobial *in vitro* activity, with MIC values

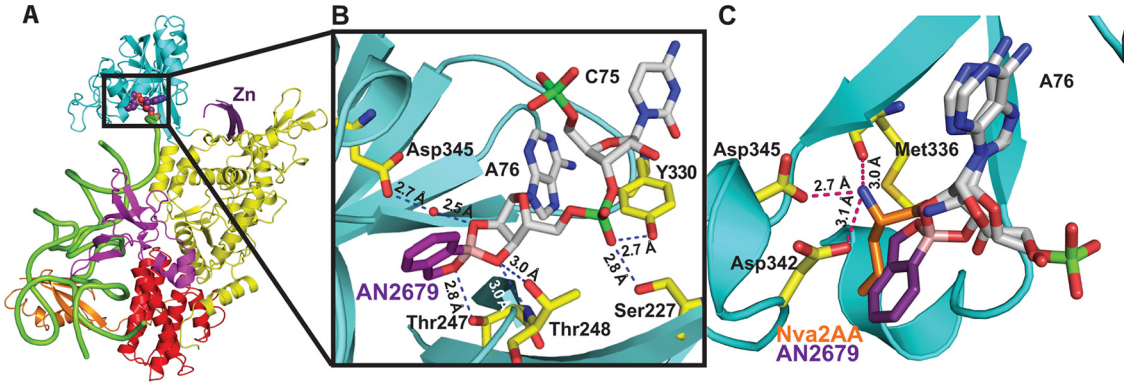

FIG 2 AN2679 LeuRS-tRNA^{Leu} cocrystal structure. (A) The 2.1-Å AN2679-*E. coli* LeuRS-tRNA^{Leu} cocrystal structure. The diagram shows the catalytic domain (yellow), editing domain (cyan), zinc domain (Zn; dark purple, partially disordered), leucyl-specific domain (mauve), anticodon-binding domain (red), C-terminal domain (orange), and tRNA (green tube). The AN2679-AMP adduct is shown in sphere representation in the editing active site. (B) Diagram of the AN2679-tRNA^{Leu} adduct, showing the ribonucleotides A76 and C75 and interacting residues. (C) An overlay of AN2679-AMP and the editing substrate analogue Nva2aa.

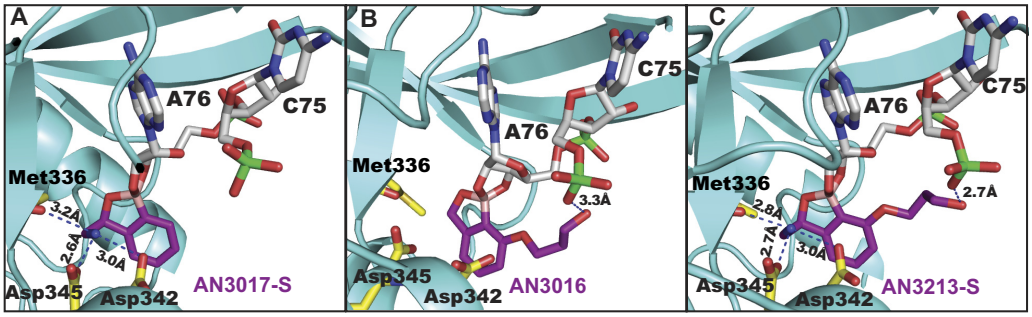

FIG 3 Compound-LeuRS-tRNA^{Leu} cocrystal structure of editing active site. (A) Diagram showing hydrogen bonds between editing site residues of LeuRS and the 3-aminomethyl group of AN3017S (purple); (B) diagram showing a hydrogen bond between the phosphate of the ribonucleotide A76 and the 7-*O*-propanol group of AN3016; (C) diagram showing hydrogen bonds formed by the 3-aminomethyl and the 7-*O*-propanol groups of AN3213S with editing site residues of LeuRS and the A76 phosphate of the tRNA.

of 1 to 2 μg/ml, compared to that of a small Gram-negative bacterial screening panel containing *E. coli*, *Klebsiella pneumonia*, and *Pseudomonas aeruginosa* (Table 2). Furthermore, no significant change in MIC values was observed for a *P. aeruginosa* strain which had the genes for three of the major efflux pumps (MexAB-OprM, MexCD-OprJ, MexEF-oprN) deleted. Likewise, no change in MIC values was observed for a strain of *E. coli* when the efflux-related *tolC* gene was disrupted by a Tn*10* insertion (Table 2).

Additional tRNA interactions improve activity. Although AN3334 was efficacious in a neutropenic mouse infection model of *E. coli* and *P. aeruginosa* (see Fig. S1 in the supplemental material), it lacked *in vitro* activity against *Proteus mirabilis* and *Acinetobacter baumannii* (Table 2). Therefore, we explored the chemical space around AN3334 in an attempt to improve activity against these bacterial species. Intriguingly, the addition of an *O*-propanol to position 7 on AN2679, which yielded AN3016, improved IC_{50} values more than 10-fold against the *E. coli* LeuRS enzyme (Fig. 1) and reduced the MIC for *A. baumannii* ATCC 15473 to 4 μg/ml (Table 2). The cocrystal structure of AN3016 with *E. coli* LeuRS-tRNA^{Leu} suggested that the hydroxy group from the *O*-propanol substituent could make a hydrogen bond interaction to the phosphate backbone of cytosine 75 of tRNA^{Leu} (Fig. 3B), which implied that interactions with the phosphate backbone of tRNA^{Leu} in addition to those with the boron-ribose adduct of adenosine 76 should yield further improvements in biochemical potency. On this basis, we synthesized AN3213 (Fig. 1), which combined the 3-aminomethyl and 7-*O*-propanol substitutions into one molecule. When AN3213 was cocrystallized with *E. coli* LeuRS and tRNA^{Leu}, it showed the combined interactions of both AN3017 and AN3016. As with AN3017, only the *S*-stereoisomer of AN3213 was bound in the editing active site (Fig. 3C). Although we added both the 3-aminomethyl and tRNA interactions, the IC_{50} of AN3213 for the *E. coli* enzyme was only 4-fold better than AN3016 and AN3017 (Fig. 1). Since we have previously shown that tavaborole was a slow, tight-binding inhibitor with *Saccharomyces cerevisiae* LeuRS (12), we tested whether these inhibitors had similar kinetics with *E. coli* LeuRS. We preincubated the *E. coli* LeuRS enzyme with tRNA and compound for different periods of time (Table 3) and found that the IC_{50} for AN2679 and AN3016 did not change with increasing preincubation times. However, the IC_{50} for AN3334 and AN3213 significantly improved with prolonged preincubation, and after preincubating AN3213 with LeuRS and tRNA for 60 min, its IC_{50} was greater than 10-fold better than that for AN3016 (Table 3). To corroborate these data, we determined the reactivation rates by measuring the time it took for *E. coli* LeuRS to recover its activity after dilution of the LeuRS-tRNA-compound inhibitor complex. It took 963 min for half of the LeuRS activity to recover after exposure with AN3213, whereas it took only 360 min with AN3334 (Table 3). Therefore, as predicted from the X-ray cocrystal structure, the addition of the 7-*O*-propanol substitution to the 3-aminomethyl benzoxaborole contributed to the biochemical potency.

In order to obtain the active enantiomer of AN3213, a synthetic intermediate was subjected to chiral HPLC separation, which led to the purification of AN3365 and AN3377 (Fig. 1). AN3365 was

TABLE 2 *In vitro* activity of benzoxaboroles against Gram-negative bacteria[a]

Organism	MIC (μg/ml)		
	AN3334	AN3016	AN3365
E. coli K12 Δ*lacU169* strain	1	8	2
E. coli K12 Δ*lacU16 tolC*::Tn*10* strain	2	2	2
E. coli ATCC 25922	1	4	1
E. coli ESBL (CTX-M-2, OXA-2)	1	16	1
K. pneumoniae 1534 (KPC-2)	0.5	16	1
E. cloacae BAA-1143 (AmpC$^+$)	1	8	0.5
P. mirabilis BAA-663 (TEM-89)	>64	32	1
P. aeruginosa PA01	2	>64	1
P. aeruginosa PAM 1626 (pump$^-$)	1	8	0.5
P. aeruginosa ATCC 27853	1	>64	4
A. baumannii ATCC 15473	>64	4	1

[a] *E. cloacae* BAA-1143 (28) is a constitutive overproducer of the class C β-lactamase AmpC. *P. aeruginosa* PAM 1626 has the three major efflux pumps deleted (29).

TABLE 3 IC_{50} from different preincubation times and reactivation rate determinations for *E. coli* LeuRS[a]

Compound	IC_{50} (μM) by preincubation period			Half-life of inhibition complex (min)
	2 min	20 min	60 min	
AN2679	ND	27.5	26.3	13
AN3016	1.5	2.1	1.8	55
AN3334	5.9	1.0	0.4	360
AN3213	2.3	0.54	0.14	963
AN3365	2.3	0.31	0.12	ND

[a] ND, not determined.

TABLE 4 Inhibition of macromolecule synthesis (EC_{50}) in *E. coli* ATCC 25922[a]

Compound	MIC (μg/ml)	EC_{50} (μg/ml)				
		Protein	RNA	DNA	Fatty acid	Cell wall
AN3365	4	8.3	105	366	396	474
Tetracycline	0.5	0.27	36	>64	>64	>64
Rifampin	8	12	12	82	>128	128
Ciprofloxacin	0.015	0.12	>0.5	0.001	>0.5	>0.5
Triclosan	≤0.004	0.18	>1	>1	0.01	>1

[a] MICs were determined in M9 minimal medium with 0.25% (wt/vol) yeast extract, and [^{14}C]leucine, [^{14}C]uridine, [^{14}C]thymidine, [^{14}C]acetic acid, and [^{14}C]*N*-acetylglucosamine incorporation was used to measure protein, RNA, DNA synthesis, fatty acid synthesis, and cell wall synthesis, respectively.

TABLE 6 AN3365 *in vitro* activity against a diverse set of bacteria

Organism	AN3365 MIC (μg/ml)
Bacteroides fragilis ATCC 25285	2
Burkholderia cepacia ATCC 25416	2
Enterococcus faecalis ATCC 29212	8
Enterococcus faecium ATCC 19434	64
Haemophilus influenzae ATCC 33391	0.5
Mycobacterium smegmatis ATCC 700084	0.25
Propionibacterium acnes ATCC 11827	8
Staphylococcus aureus ATCC 29213	4
Staphylococcus aureus ATCC 33591	8
Staphylococcus epidermidis ATCC 12228	2
Staphylococcus saprophyticus ATCC 15305	1
Stenotrophomonas maltophilia ATCC 13637	1
Streptococcus pneumoniae ATCC 6301	2
Streptococcus pyogenes ATCC 19615	2

the active enantiomer and was 150-fold more potent than AN3377 against the *E. coli* LeuRS enzyme, with an IC_{50} of 0.31 μM (Fig. 1). Since the core benzoxaborole, AN2679, has antifungal activity, we determined the bacterium specificity of the lead compound. AN3365 had no activity against the yeasts *Candida glabrata* ATCC 90030 and *Candida albicans* ATCC 90028, with MIC values of >64 μg/ml, and it had poor activity versus a human hepatocellular carcinoma cell line (HepG2) and human cytoplasmic LeuRS, with IC_{50} values of >500 μM and 185 μM, respectively. When AN3365 was tested against a screening panel of *E. coli*, *K. pneumoniae*, *Enterobacter cloacae*, and *P. aeruginosa*, we observed MIC values ranging from 0.5 to 4 μg/ml (Table 2). MIC values against the efflux-deficient bacteria *E. coli tolC*::Tn*10* and *P. aeruginosa* (Δ*mexAB-oprM* Δ*mexCD-oprJ* Δ*mexEF-oprN*) were not significantly different from those of the wild-type strains, which suggests that AN3365 is not notably affected by these efflux mechanisms in *E. coli* and *P. aeruginosa* (Table 2).

To confirm that AN3365 specifically inhibited protein synthesis, we determined its effect on the major biosynthetic pathways in *E. coli* ATCC 25922. The half-maximal effective concentration (EC_{50}) for protein synthesis inhibition was within error of its MIC in minimal M9 medium plus 0.25% (wt/vol) yeast extract, which we used to facilitate incorporation of ^{14}C-leucine into protein (Table 4). This behavior was similar to the effect that was observed with the protein synthesis inhibitor tetracycline but was very different from that observed with antibiotics that have other primary targets, namely, rifampin, ciprofloxacin, and triclosan (Table 4). These data confirm that the observed antibacterial activity of AN3365 is due to selective inhibition of protein biosynthesis.

***In vitro* activity of AN3365 against multidrug-resistant Gram-negative bacterial isolates.** Since the largest unmet medical need for new antibacterials is the treatment of multidrug-resistant (MDR) Gram-negative bacterial infections, we tested AN3365 against a small panel of MDR clinical isolates of *A. baumannii*, *P. aeruginosa*, and *Enterobacteriaceae*, as well as16 isolates producing the metallo-β-lactamase NDM-1 (Table 5). AN3365 retained activity against these MDR isolates, for example, with an MIC of 2 μg/ml for the fluoroquinolone-, carbapenem-, and polymyxin B-resistant isolate *A. baumannii* BAA-1605 (see Table S1 in the supplemental material). No loss of activity was observed for any members of a panel of 11 *P. aeruginosa* strains, including isolates with metallo-β-lactamases, AmpC overexpression, or a mutation in the porin gene *oprD* (see Table S2 in the supplemental material). MIC values for 19 *Enterobacteriaceae* isolates and 16 additional isolates with the NDM-1 enzyme all fell within a narrow MIC range, from 0.5 to 2 μg/ml (Table 5), and no significant resistance was observed even for an *Enterobacteriaceae* isolate with outer membrane permeability mutations (see Table S3 in the supplemental material). This was not the case for the standard antibiotics ciprofloxacin, levofloxacin, ceftazidime, meropenem, polymyxin B, and tigecycline or tobramycin, which were all compromised (Tables 5). However, testing of larger collections of isolates will be necessary to fully confirm the spectrum and antibacterial activity of AN3365. AN3365 was also tested against single isolates of a wider set of bacteria, revealing activity against the Gram-negative anaerobe *Bacteroides fragilis* and some Gram-positive bacteria (Table 6).

***In vivo* efficacy against Gram-negative bacterial infections.** The pharmacokinetics of AN3365 were determined in mice to ensure that plasma levels were sufficient to perform *in vivo*

TABLE 5 *In vitro* activity of AN3365 and comparators against multidrug-resistant Gram-negative bacteria[a]

Organism (no. of isolates)	MIC (μg/ml)					
	AN3365		Ciprofloxacin		Meropenem	
	Range	90%	Range	90%	Range	90%
A. baumannii (16)	0.5–4	4	0.12–>64	>64	4–>64	>64
Enterobacteriaceae (18)	0.5–2	2	≤0.006–>6.4	>6.4	≤0.06–>64	64
Enterobacteriaceae NDM-1 (16)	0.5–2	2	0.03–>16[b]	>16[b]	≤0.0-6–>64	64
P. aeruginosa (11)	1–4	4	0.12–>64	>64	0.25–>64	>64

[a] MIC values were determined using M7-A7 CLSI guidelines for aerobic bacteria (27). The MIC_{90} is the concentration that inhibits 90% of the isolates.
[b] The fluoroquinolone levofloxacin was tested instead of ciprofloxacin; these compounds have similar activities and near-complete cross-resistance against Gram-negative bacteria. The levofloxacin and meropenem MIC values in the NDM-1 panel were determined by the agar dilution method of the British Society for Antimicrobial Chemotherapy.

TABLE 7 AN3365 murine pharmacokinetic parameters

Parameter[a]	Value
i.v. (30 mg/kg)[b]	
C_{max} (μg/ml) at 5 min	26.0
CL (ml/h/kg)	2914
Vc (ml/kg)	805
Vss (ml/kg)	3895
MRT (h)	1.34
AUC (h · μg/ml)	10.3
α-$t_{1/2}$ (h) (% AUC)	0.12 (62)
β-$t_{1/2}$ (h) (% AUC)	2.23 (38)
p.o. (30 mg/kg)[c]	
C_{max} (μg/ml)	0.90
T_{max} (h)	0.5
AUC_{last} (h · μg/ml)	2.2
Terminal $t_{1/2}$ (h)	2.7
% bioavailability	21
% plasma protein binding	7.6
s.c. (30 mg/kg)[c]	
C_{max} (μg/ml)	8.4
T_{max} (h)	0.25
AUC_{last} (h · μg/ml)	12.1
Terminal $t_{1/2}$ (h)	2.5
% bioavailability	100

[a] CL, clearance; Vc, volume of distribution of central compartment; Vss, volume of distribution at steady state; MRT, mean residence time; α-$t_{1/2}$, alpha-phase half-life; β-$t_{1/2}$, beta-phase phase half-life; T_{max}, time to maximum drug concentration; Terminal $t_{1/2}$, half-life of the drug after reaching pseudo-equilibrium.
[b] WinNonlin two-compartment analysis with $1/y^2$ weighting.
[c] WinNonlin noncompartment analysis with uniform weighing.

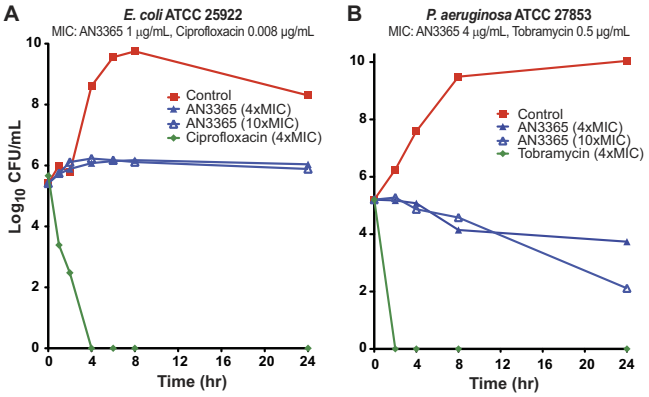

FIG 5 *In vitro* antibacterial kinetics of AN3365. (A) The viability of *E. coli* ATCC 25922 over 24 h in MHB treated with AN3365 at 4-fold and 10-fold its MIC and the control ciprofloxacin at 4-fold its MIC. (B) The viability of *P. aeruginosa* ATCC 27853 over 24 h in MHB treated with AN3365 at 4-fold and 10-fold its MIC and the control tobramycin at 4-fold its MIC.

efficacy studies. When AN3365 was dosed s.c. at 30 mg/kg, it achieved plasma exposures with an AUC_{last} of 12.1 h · μg/ml and a maximum concentration of drug in serum (C_{max}) of 8.4 μg/ml (Table 7). Based on this plasma exposure and half-life, AN3365 was administered s.c. either twice a day (BID) or once a day (QD) at 30 mg/kg in a 24-h neutropenic murine thigh infection model. These dose regimes achieved results similar to 20 mg/kg of tobramycin s.c. against *E. coli* ATCC 25922 (Fig. 4A). Predictably, AN3365 was more effective than tobramycin against an aminoglycoside-resistant strain of *E. coli*, ANA 589, which also produced an extended-spectrum β-lactamase (ESBL) (Fig. 4B). AN3365 demonstrated similar efficacy to tobramycin when administered s.c. against *P. aeruginosa* ATCC 27853 (Fig. 4C). Although AN3365 is only 21% orally bioavailable in mice (Table 7), we decided to test its oral efficacy against *P. aeruginosa* 1161949 in a 4-day immunocompetent murine thigh infection model. When AN3365 was dosed at 75 mg/kg BID, it gave a 1.6 log_{10} CFU reduction from the 1-h control, while 300 mg/kg BID gave more than a 3 log_{10} CFU reduction from the 1-h control (Fig. 4D).

Kinetics of *in vitro* activity. Aminoacyl-tRNA synthetase inhibitors are bacteriostatic agents (30); thus, the bacteriostatic activity of AN3365 with *E. coli* ATCC 25922 was to be expected (Fig. 5A). However, the kinetics with *P. aeruginosa* ATCC 27853 were very different, as the number of colonies dropped by 1.5 log_{10} CFU/ml and 3.1 log_{10} CFU/ml over 24 h when exposed to 4-fold MIC and 10-fold MIC, respectively (Fig. 5B). Testing of additional *P. aeruginosa* isolates will be necessary to determine if this is a species- or strain-specific effect.

Antipseudomonal mechanism of action. All previous AARS

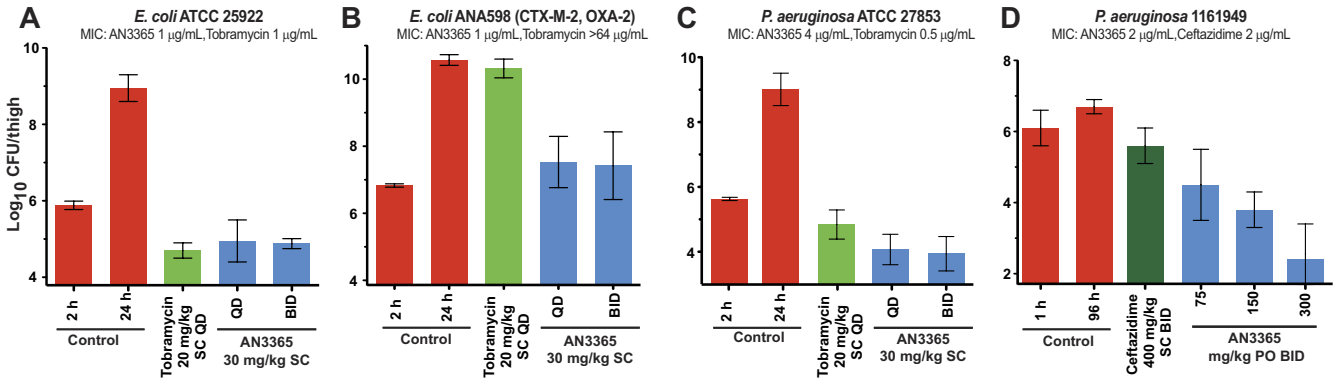

FIG 4 AN3365 mouse *in vivo* efficacy. (A) AN3365 dosed subcutaneously in a neutropenic mouse thigh infection model of *E. coli* ATCC 25922; (B) AN3365 dosed subcutaneously in a neutropenic mouse thigh infection model using the aminoglycoside-resistant *E. coli* ANA598 strain with CTX-M-2 and OXA-2 β-lactamases; CTX-M-2 is an extended-spectrum β-lactamase (ESBL); (C) AN3365 dosed subcutaneously in a neutropenic mouse thigh infection model of *P. aeruginosa* ATCC 27853; (D) AN3365 dosed orally in a 4-day immunocompetent mouse thigh infection model of *P. aeruginosa* 1161949. Mean log_{10} CFU/ml and standard deviations from four to six mice were plotted for each time point. Only 7.6% of AN3365 is bound to plasma protein in mice.

TABLE 8 Single-step resistance frequency for *P. aeruginosa* ATCC 27853

Antibiotic	MIC (μg/ml)	Concn selected (MIC multiple)	Resistance frequency
AN3365	4	4-fold	1.2×10^{-7}
		10-fold	4.8×10^{-8}
Ceftazidime	2	4-fold	2.9×10^{-7}
		10-fold	2.6×10^{-7}
Ciprofloxacin	0.25	4-fold	2.0×10^{-7}
		10-fold	$<2.8 \times 10^{-9}$
Tobramycin	0.5	4-fold	5.5×10^{-7}
		10-fold	8.3×10^{-9}

TABLE 9 Single-step resistance frequency for isolates of *E. coli* and *K. pneumoniae*

Antibiotic	MIC (μg/ml)	Concn selected (MIC multiple)	Resistance frequency[a]
E. coli OXA-1, SHV-5			
AN3365	1	4-fold	1.3×10^{-7}
		10-fold	7.5×10^{-8}
Ceftazidime	>16	4-fold	ND
		10-fold	ND
Meropenem	1	4-fold	ND
		10-fold	ND
K. pneumoniae ATCC 13883			
AN3365	1	4-fold	8.1×10^{-7}
		10-fold	6.1×10^{-8}
Ceftazidime	0.25	4-fold	$\sim 10^{-6}$
		10-fold	$\sim 10^{-6}$
Meropenem	0.06	4-fold	$<2.5 \times 10^{-9}$
		10-fold	$<2.5 \times 10^{-9}$
K. pneumoniae ATCC 51503			
AN3365	1	4-fold	5.3×10^{-8}
		10-fold	3.8×10^{-8}
Ceftazidime	>16	4-fold	ND
		10-fold	ND
Meropenem	0.5	4-fold	4.8×10^{-7}
		10-fold	$<3.7 \times 10^{-9}$

[a] ND, not determined.

inhibitors are bacteriostatic agents (30, 31) and they inhibit AARS enzymes by binding to the synthetic active site, whereas the aminomethylbenzoxaboroles block tRNA aminoacylation by trapping the tRNA in the editing conformation. Since the levels of the respective AARS and their cognate tRNA are tightly regulated to avoid mischarging (32), it is plausible that the sequestration of $tRNA^{Leu}$ on LeuRS might generate a different response to that observed with previous AARS inhibitors. Conversely, the slow bactericidal activity observed against *P. aeruginosa* ATCC 27853 at 10-fold the MIC could be due to off-target activity. Therefore, we sought to confirm the specificity of AN3365's mechanism of action using a genetic approach. To this end, we selected for AN3365-resistant mutants of *P. aeruginosa* ATCC 27853 at 4-fold and 10-fold its MIC value on Mueller-Hinton agar (MHA) and obtained single-step resistance frequencies of 1.2×10^{-7} and 4.8×10^{-8}, respectively (Table 8). These resistance frequencies were comparable to those obtained with *E. coli* and *K. pneumoniae* isolates (Table 9). Also, the frequency of resistance was not that different from that published for fosfomycin with *E. coli* (33) and tigecycline with *K. pneumoniae* (34). However, resistance frequency is still on the high side; therefore, a potential risk exists for development of AN3365.

Although the AN3365-resistant mutants of *P. aeruginosa* ATCC 27853 had MIC values for AN3365 of 32 μg/ml and greater, these mutants did not show any changes in MIC values for any of the comparators, for example, ciprofloxacin, ceftazidime, gentamicin, tobramycin, or polymyxin B. To determine if the resistance mutation resided in the gene for LeuRS, we picked 10 resistant colonies and sequenced *leuS*. All 10 mutants bore a mutation in the editing active site of LeuRS; five had a missense mutation that would result in a Thr256Pro change, whereas four had a Val342Met change and one had a Thr252Pro change.

Mutations in the editing active site confer norvaline sensitivity. Since these mutations resided in the editing active site of LeuRS, we decided to test whether they conferred sensitivity to a close analogue of leucine. Although LeuRS can aminoacylate $tRNA^{Leu}$ with norvaline (22), its editing active site hydrolyzes the norvaline-charged $tRNA^{Leu}$, thereby ensuring the fidelity of protein synthesis. All the AN3365-resistant mutants were found to be sensitive to norvaline when grown in M9 glucose minimal medium, with an MIC of 4 μg/ml for the *leuS* Thr256Pro mutant and 0.25 μg/ml for the *leuS* Val342Met and Thr252Pro mutants, compared with >64 μg/ml for the *P. aeruginosa* ATCC 27853 parental strain. Since these mutants were sensitive to norvaline, it is likely they are editing defective (22). This acute sensitivity to norvaline might explain why the editing activity is maintained in most organisms, for example, when glucose-grown *E. coli* isolates are subjected to downshifts in oxygen tension, they produce millimolar amounts of norvaline (35). As for human pathogens, it is unclear how much selective pressure norvaline, which is a natural human metabolite (36), exerts to maintain editing function. However, in some circumstances, editing function can be dispensed with where the leucine concentration is significantly above the level of norvaline or the LeuRS synthetic site has improved specificity, for example, the organelles, the mammalian mitochondria (37), and the malarial apicoplast (38), and with MHB where the leucine concentration is approximately 6 mM, which is at least 30-fold higher than the normal human physiological level of 56 to 203 μM (39). So far, the only free-living organism that has been convincingly shown to have totally lost its LeuRS editing function is *Mycoplasma mobile* (40).

AN3365 is on target in *P. aeruginosa*. In order to confirm that a mutation in *leuS* confers resistance to AN3365, we reintroduced the Thr252Pro mutation into *P. aeruginosa* ATCC 27853 using an *sacB*-mediated allelic replacement method (25). AN3365 and norvaline MIC values for *P. aeruginosa* ATCC 27853 bearing this mutation were >64 and 0.25 μg/ml, respectively. We conclude that mutations in *leuS* do confer resistance to AN3365; therefore, the slow bactericidal activity observed at 10-fold MIC in this strain of *P. aeruginosa* is most likely due to on-target inhibition of LeuRS.

In conclusion, AN3365 is representative of a novel class of antibacterials containing boron, the aminomethylbenzoxaboroles, which inhibit a novel target, the editing site of leucyl-tRNA synthetase. Through a combination of inhibiting a novel target and favorable physical chemical properties, AN3365 largely circum-

vents the major efflux mechanisms, suggesting that it could address the pressing unmet medical need of treating multidrug-resistant Gram-negative bacterial infections. However, in spite of therapeutic responses (resolution of clinical signs and symptoms and clearance of baseline pathogen from the urine) being observed in the recent phase 2 trial for complicated urinary tract infections (cUTI), the study was stopped early in enrolment due to emergence of AN3365 resistance in bacterial isolates from a subpopulation of patients. The concomitant complicated intra-abdominal phase 2 trial was also stopped due to this microbiological finding in the cUTI trial (John Tomayko, personal communication). Further work is continuing to find ways to circumvent this problem to enable its further progression in the clinic.

ACKNOWLEDGMENTS

We thank Jurene Fong and Maureen Kully for initial microbial experiments, Joana Antunes for *in vitro* cytotoxicity studies, Georgia Musetescu for compound management, Susan Martinis for a kind gift of *E. coli* LeuRS, and Inderjit Sidhu for the chiral HPLC analysis of compounds. Furthermore, we thank Huchen Zhou, Annie Xia, Myung-Gi Baek, Chris Diaper, Chan Ha, Leroy Lu, Rahim Mohammad, Jim Phillips, and Neil Pearson for their contributions to medicinal chemistry. EMBL thanks the ESRF-EMBL Joint Structural Biology group for access to ESRF beamlines. Lastly, we thank Steve Benkovic and Lucy Shapiro for their help and support.

REFERENCES

1. **European Centre for Disease Prevention and Control.** 2010. Antimicrobial resistance surveillance in Europe 2009. Annual report of the European Antimicrobial Resistance Surveillance Network (EARS-Net). ECDC, Stockholm, Sweden.
2. **Gagliotti C, Balode A, Baquero F, Degener J, Grundmann H, Gur D, Jarlier V, Kahlmeter G, Monen J, Monnet DL, Rossolini GM, Suetens C, Weist K, Heuer O.** 2011. *Escherichia coli* and *Staphylococcus aureus*: bad news and good news from the European Antimicrobial Resistance Surveillance Network (EARS-Net, formerly EARSS), 2002 to 2009. Euro Surveill. **16**:pii=19819.
3. **Rhomberg PR, Jones RN.** 2009. Summary trends for the Meropenem Yearly Susceptibility Test Information Collection Program: a 10-year experience in the United States (1999-2008). Diagn. Microbiol. Infect. Dis. **65**:414–426.
4. **Peleg AY, Hooper DC.** 2010. Hospital-acquired infections due to Gram-negative bacteria. N. Engl. J. Med. **362**:1804–1813.
5. **Walsh TR, Weeks J, Livermore DM, Toleman MA.** 2011. Dissemination of NDM-1 positive bacteria in the New Delhi environment and its implications for human health: an environmental point prevalence study. Lancet Infect. Dis. **11**:355–362.
6. **Nordmann P, Cuzon G, Naas T.** 2009. The real threat of *Klebsiella pneumoniae* carbapenemase-producing bacteria. Lancet Infect. Dis. **9**:228–236.
7. **Livermore DM, Warner M, Mushtaq S, Doumith M, Zhang J, Woodford N.** 2011. What remains against carbapenem-resistant *Enterobacteriaceae*? Evaluation of chloramphenicol, ciprofloxacin, colistin, fosfomycin, minocycline, nitrofurantoin, temocillin and tigecycline. Int. J. Antimicrob. Agents **37**:415–419.
8. **Li J, Nation RL, Turnidge JD, Milne RW, Coulthard K, Rayner CR, Paterson DL.** 2006. Colistin: the re-emerging antibiotic for multidrug-resistant Gram-negative bacterial infections. Lancet Infect. Dis. **6**:589–601.
9. **Neonakis IK, Samonis G, Messaritakis H, Baritaki S, Georgiladakis A, Maraki S, Spandidos DA.** 2010. Resistance status and evolution trends of *Klebsiella pneumoniae* isolates in a university hospital in Greece: ineffectiveness of carbapenems and increasing resistance to colistin. Chemotherapy **56**:448–452.
10. **Drapeau CM, Grilli E, Petrosillo N.** 2010. Rifampicin combined regimens for Gram-negative infections: data from the literature. Int. J. Antimicrob. Agents **35**:39–44.
11. **Sutherland R, Boon RJ, Griffin KE, Masters PJ, Slocombe B, White AR.** 1985. Antibacterial activity of mupirocin (pseudomonic acid), a new antibiotic for topical use. Antimicrob. Agents Chemother. **27**:495–498.
12. **Rock FL, Mao W, Yaremchuk A, Tukalo M, Crepin T, Zhou H, Zhang YK, Hernandez V, Akama T, Baker SJ, Plattner JJ, Shapiro L, Martinis SA, Benkovic SJ, Cusack S, Alley MR.** 2007. An antifungal agent inhibits an aminoacyl-tRNA synthetase by trapping tRNA in the editing site. Science **316**:1759–1761.
13. **Hendrickson TL, Schimmel P.** 2003. Transfer RNA-dependent amino acid discrimination by aminoacyl-tRNA synthetase. Landes Bioscience/Eurekah.com, Austin, TX.
14. **Lincecum TL, Jr, Tukalo M, Yaremchuk A, Mursinna RS, Williams AM, Sproat BS, Van Den Eynde W, Link A, Van Calenbergh S, Grotli M, Martinis SA, Cusack S.** 2003. Structural and mechanistic basis of pre- and posttransfer editing by leucyl-tRNA synthetase. Mol. Cell **11**:951–963.
15. **Palencia A, Crepin T, Vu MT, Lincecum TL, Jr, Martinis SA, Cusack S.** 2012. Structural dynamics of the aminoacylation and proofreading functional cycle of bacterial leucyl-tRNA synthetase. Nat. Struct. Mol. Biol. **19**:677–684.
16. **Kabsch W.** 2010. Xds. Acta Crystallogr. D Biol. Crystallogr. **66**:125–132.
17. **Winn MD, Ballard CC, Cowtan KD, Dodson EJ, Emsley P, Evans PR, Keegan RM, Krissinel EB, Leslie AG, McCoy A, McNicholas SJ, Murshudov GN, Pannu NS, Potterton EA, Powell HR, Read RJ, Vagin A, Wilson KS.** 2011. Overview of the CCP4 suite and current developments. Acta Crystallogr. D Biol. Crystallogr. **67**:235–242.
18. **McCoy AJ, Grosse-Kunstleve RW, Adams PD, Winn MD, Storoni LC, Read RJ.** 2007. Phaser crystallographic software. J. Appl. Crystallogr. **40**:658–674.
19. **Emsley P, Lohkamp B, Scott WG, Cowtan K.** 2010. Features and development of Coot. Acta Crystallogr. D Biol. Crystallogr. **66**:486–501.
20. **Murshudov GN, Vagin AA, Dodson EJ.** 1997. Refinement of macromolecular structures by the maximum-likelihood method. Acta Crystallogr. D Biol. Crystallogr. **53**:240–255.
21. **Ling C, Yao YN, Zheng YG, Wei H, Wang L, Wu XF, Wang ED.** 2005. The C-terminal appended domain of human cytosolic leucyl-tRNA synthetase is indispensable in its interaction with arginyl-tRNA synthetase in the multi-tRNA synthetase complex. J. Biol. Chem. **280**:34755–34763.
22. **Martinis SA, Fox GE.** 1997. Non-standard amino acid recognition by *Escherichia coli* leucyl-tRNA synthetase. Nucleic Acids Symp. Ser. (Oxf.) **36**:125–128.
23. **CLSI.** 2006. Methods for dilution antimicrobial susceptibility tests for bacteria that grow aerobically; approved standard—7th edition. CLSI document M7-A7, vol 2. Clinical and Laboratory Standards Institute, Wayne, PA.
24. **CLSI.** 2007. Methods for antimicrobial susceptibility testing of anaerobic bacteria: approved standard—7th ed. Clinical and Laboratory Standards Institute, Wayne, PA.
25. **Edwards RA, Keller LH, Schifferli DM.** 1998. Improved allelic exchange vectors and their use to analyze 987P fimbria gene expression. Gene **207**:149–157.
26. **McGowan SJ, Gorham HC, Hodgson DA.** 1993. Light-induced carotenogenesis in *Myxococcus xanthus*: DNA sequence analysis of the *carR* region. Mol. Microbiol. **10**:713–735.
27. **Figurski DH, Helinski DR.** 1979. Replication of an origin-containing derivative of plasmid RK2 dependent on a plasmid function provided in *trans*. Proc. Natl. Acad. Sci. U. S. A. **76**:1648–1652.
28. **Gootz TD, Sanders CC, Goering RV.** 1982. Resistance to cefamandole: derepression of beta-lactamases by cefoxitin and mutation in *Enterobacter cloacae*. J. Infect. Dis. **146**:34–42.
29. **Griffith DC, Corcoran E, Lofland D, Lee A, Cho D, Lomovskaya O, Dudley MN.** 2006. Pharmacodynamics of levofloxacin against *Pseudomonas aeruginosa* with reduced susceptibility due to different efflux pumps: do elevated MICs always predict reduced *in vivo* efficacy? Antimicrob. Agents Chemother. **50**:1628–1632.
30. **Critchley IA, Young CL, Stone KC, Ochsner UA, Guiles J, Tarasow T, Janjic N.** 2005. Antibacterial activity of REP8839, a new antibiotic for topical use. Antimicrob. Agents Chemother. **49**:4247–4252.
31. **Hurdle JG, O'Neill AJ, Chopra I.** 2005. Prospects for aminoacyl-tRNA synthetase inhibitors as new antimicrobial agents. Antimicrob. Agents Chemother. **49**:4821–4833.
32. **Sherman JM, Rogers MJ, Soll D.** 1992. Competition of aminoacyl-tRNA synthetases for tRNA ensures the accuracy of aminoacylation. Nucleic Acids Res. **20**:2847–2852.
33. **Nilsson AI, Berg OG, Aspevall O, Kahlmeter G, Andersson DI.** 2003.

Biological costs and mechanisms of fosfomycin resistance in *Escherichia coli*. Antimicrob. Agents Chemother. **47**:2850–2858.
34. **Ruzin A, Visalli MA, Keeney D, Bradford PA.** 2005. Influence of transcriptional activator RamA on expression of multidrug efflux pump AcrAB and tigecycline susceptibility in *Klebsiella pneumoniae*. Antimicrob. Agents Chemother. **49**:1017–1022.
35. **Soini J, Falschlehner C, Liedert C, Bernhardt J, Vuoristo J, Neubauer P.** 2008. Norvaline is accumulated after a down-shift of oxygen in *Escherichia coli* W3110. Microb. Cell Fact. **7**:30.
36. **Guo K, Li L.** 2009. Differential 12C-/13C-isotope dansylation labeling and fast liquid chromatography/mass spectrometry for absolute and relative quantification of the metabolome. Anal. Chem. **81**:3919–3932.
37. **Lue SW, Kelley SO.** 2007. A single residue in leucyl-tRNA synthetase affecting amino acid specificity and tRNA aminoacylation. Biochemistry (Mosc.) **46**:4466–4472.
38. **Khan S, Sharma A, Jamwal A, Sharma V, Pole AK, Thakur KK, Sharma A.** 2011. Uneven spread of *cis*- and *trans*-editing aminoacyl-tRNA synthetase domains within translational compartments of *P. falciparum*. Sci. Rep. **1**:188.
39. **Tan IK, Gajra B.** 2006. Plasma and urine amino acid profiles in a healthy adult population of Singapore. Ann. Acad. Med. Singapore. **35**:468–475.
40. **Boniecki MT, Martinis SA.** 2012. Coordination of tRNA synthetase active sites for chemical fidelity. J. Biol. Chem. **287**:11285–11289.